Investigation of Acoustic Streaming in a Thermoacoustic-Stirling Heat Engine

Duthil P., Bretagne E., Wu J., François M.-X., Li Q.*.

LIMSI-CNRS, BP 133, 91403 Orsay Cedex, France
*Technical Institute of Physics and Chemistry, CAS, Beijing 100080, China

Experimental characterization of acoustic streaming in a thermoacoustic-Stirling heat engine is presented. Investigation is indeed carried out with and without Gedeon streaming suppression by means of a rubber balloon positioned inside the loop at a given place. First, results show that whereas the temperature distribution in the regenerator is weakly affected by the streaming flow, heat fluxes measured in the heat exchangers determines the direction of this acoustic streaming. Moreover, they reveal that additional thermal effects are coupled with the streaming. Finally, they show that thermoacoustic conversion efficiency is improved by inserting the rubber balloon.

INTRODUCTION

Gedeon [1] has been concerned with how nonzero second order steady mass flow can arise in Stirling and pulse tube crycoolers whenever a closed-loop path exists. Later on, the term Gedeon streaming has been used [2] to describe such DC flow in the case of a close-loop flow path existing within the device. Theoretical studies of acoustic streaming were extended to annular thermoacoustic prime-mover [3] as well as to channels of arbitrary width in a standing wave [4]. Recent experiments [5-7] confirm the existence of the closed-loop streaming. Moreover, it was demonstrated that suppression of the streaming significantly increases the efficiency of the device. It is interesting to note that some research groups [8-11] study indirectly acoustic streaming through the analysis of jet pumps.

In the current paper, we focus on the Gedeon streaming existence and direction in thermoacoustic-Stirling heat engine through the analyses of temperature profile in the regenerator and heat fluxes in the heat exchangers.

APPARATUS

A thermoacoustic-Stirling heat engine has been designed. A scale drawing of the loop section of the experimental apparatus is shown in Figure 1, without the resonator section - similar to that of [6]. The loop section contains the heat exchangers and the regenerator. We describe briefly the core of the apparatus. Near the top of the loop is the cold heat exchanger. It is made of shell-and-tube construction consisting of 95 brass tubes of 3 mm inside diameter and 35 mm long, welded into a copper flange. The total gas-solid contact area is of 0.0313 m^2. Below the cold heat exchanger is the 75 mm long regenerator which is made of a stainless-steel screens stack [12] machined to a diameter of 56.3mm. The lower end of the regenerator abuts the hot heat exchanger. It is a copper screens stack; the heater is made of six 1-mm-diameter electrically insulated wire [13] with a total resistance of $10\,\Omega$. The thermal buffer tube (TBT) is an upper straight cylinder flaring along its lower part with a 1.35° half-angle taper. This taper is used to minimize boundary layer driven streaming (Rayleigh streaming) [14]. At the lower end of the TBT is another cold heat exchanger of same design as the cold heat exchanger previously described, but of 20-mm-length and 0.0179m^2 total gas-solid contact area.

9 type-K thermocouples allow the measurement of the axial temperature profile within the regenerator and the water temperature flowing in/out of the two cold heat exchangers. Absolute accuracy of the thermocouples is of 0.1K but preliminary tests in purely conductive state (mainly linear temperature profile) revealed an accuracy of 2% relatively to their location within the regenerator. In order to determine heat fluxes extracted through the cold heat exchangers, temperature measurements were coupled with mass flow rates measurements (double weighting method) leading to a relative accuracy of 10% on the measured heat power. The input heat power is known from the voltage and intensity of the resistive wires with an accuracy of 1W.

A piezoresistive pressure sensor located at 80mm above the cold heat exchanger allows the measurement of oscillatory pressure - labeled with p_1.

Figure 1. Scale drawing of the loop section.

To quickly confirm Gedeon streaming, we compared experimental results with and without the placement of a rubber balloon at the position shown in Figure 1: we expected the balloon to be acoustically transparent, but to completely block Gedeon streaming. Preliminary experimental work showed good reproducibility of the results for those two cases: with and without balloon.
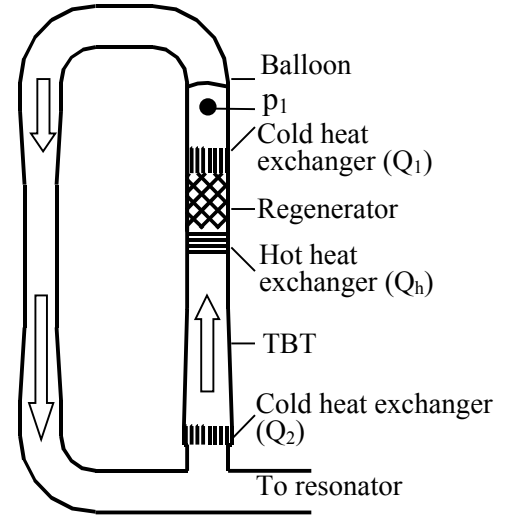
EXPERIMENTAL RESULTS

It was assumed that the temperature spatial profile along the axis of the regenerator was related to Gedeon streaming in the loop [5, 15]. Hence, in the cases of suppressing or not the Gedeon streaming, we measured the temperature profiles in the regenerator for three different mean pressures (1.1MPa, 2.0MPa and 3.0MPa) and for different input heat powers. With working gas being nitrogen, the normalized temperature $\left(T(x/L) - T_c\right)/\left(T_h - T_c\right)$ is plotted in Figure 2 and Figure 3 as a function of the normalized length x/L. Here, T_c and T_h are temperatures at the cold and hot ends of the regenerator, respectively. L is the length of the regenerator and x is axial position measured from the cold end of the regenerator. In the case of a free closed-loop path (i.e. without balloon), the normalized temperature profiles have a trend to incurve upwards for a mean pressure of 1.1MPa (input heat power ranging between 172W and 330W; pressure ratio varying from 0.48% to 1.1%) and have an opposite trend at 3.0MPa (input heat power ranging between 810W and 1150W; pressure ratio varying from 1.75% to 2.24%). As for different heat power temperature, profiles are similar for each mean pressure, only two
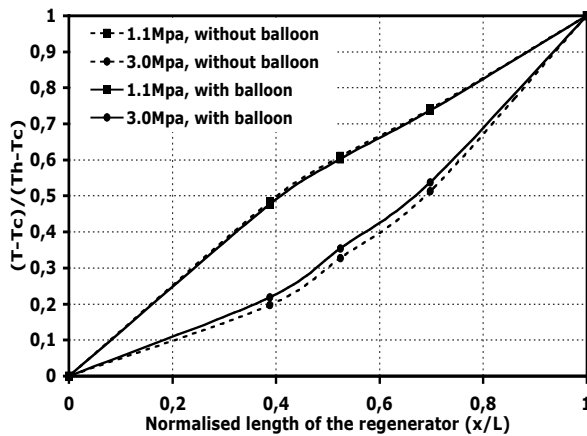

Figure 2. Normalized temperature $(T-T_c)/(T_h-T_c)$ vs normalized length x/L at 1.1MPa and 3.0MPa with (solid lines) and without (dashed lines) balloon. For each pressure, representative profile is plotted only.
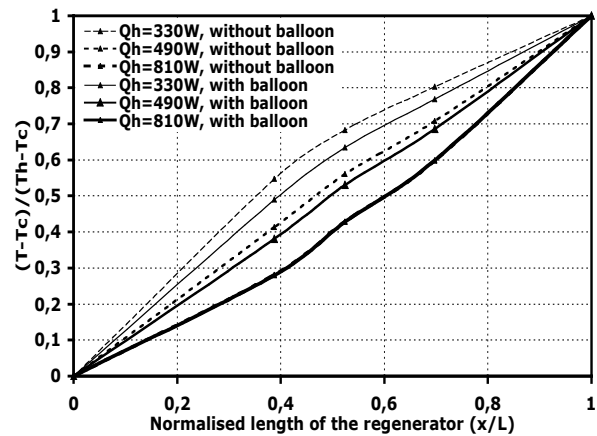
Figure 3. Normalized temperature $(T-T_c)/(T_h-T_c)$ vs normalized length x/L at 2.0MPa with (solid lines) and without (dashed lines) balloon.

representative profiles corresponding to the respective maximum powers 330W (filled squares) and 1150W (filled circles) have been plotted with dash lines in Figure 2. Similarly, in the case of balloon insertion, we plotted with solid lines in Figure 2 the temperature profiles corresponding to the same input power at the same mean pressure (330W at 1.1Mpa - filled squares and 1150W at 3.0Mpa -filled circles). Choosing an intermediate mean pressure of 2.0MPa (shown in Figure 3), the normalized temperature profiles evolve with the increase of input heat power (from 330W to 890W; drive ratio varying from 1.18% to 2.1%) from an upward curve through a nearly linear profile to a downward curve. This is true for the cases with (solid lines) and without (dash lines) balloon.

Considering the comparison between the temperature T_{mid}, at the axial midpoint of the regenerator, and the average temperature $T_{ave}=(T_c+T_h)$ as an indication for determining direction of Gedeon streaming [5,7], it should come at i) 1.1MPa, $T_{mid}>T_{ave}$, $M_2>0$ (anticlockwise through the loop), implying that the Gedeon streaming flows up in the regenerator; ii) 3.0MPa, $T_{mid}<T_{ave}$, $M_2<0$ (clockwise through the loop), implying that the Gedeon streaming flows down in the regenerator; iii) 2.0MPa, the direction of Gedeon streaming changes from anticlockwise to clockwise with the heat power. However, as illustrated in Figure 2 and Figure 3, the balloon has weak effect on the normalized temperature profiles so that Gedeon streaming does not seem to influence it. On the contrary, it seems that both the input power Q_h and the mean pressure have an obvious effect.

For those reasons, we decided to measure lost heat carried out by water flow through the two cold heat exchangers in order to determine the direction of Gedeon streaming. To obtain obvious water temperature difference between entrance and exit of cold heat exchanger, we adjust the water massflow rate to 5g/s. Lost heat powers from the two cold heat exchangers are shown in Figure 4 (a) and Figure 4 (b) where the lost heat is plotted versus the input heat power for three different mean pressure.
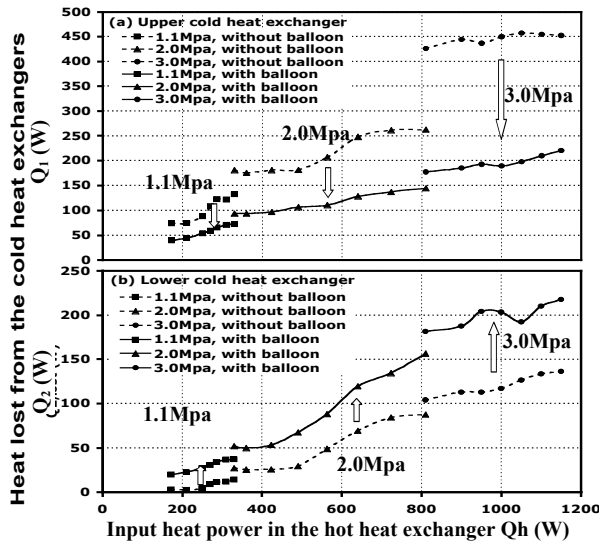

Figure 4. Lost heat power from the upper (a) and lower (b) cold heat exchangers vs input heat power for different mean pressures with (solid lines) and without (dashed lines) balloon.
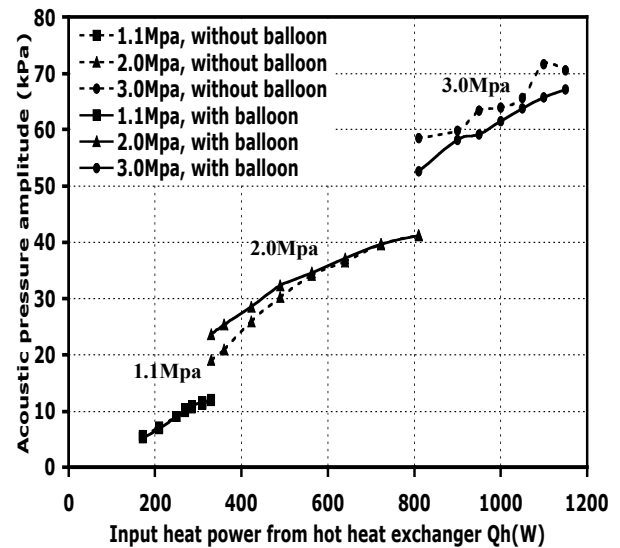
Figure 5 Dynamic pressure amplitude vs input heat power for different mean pressures with (solid lines) and without (dashed lines) balloon.

Here, subscripts 1 and 2 denote for the upper and lower cold heat exchangers respectively (cf. Figure 1). Solid and dashed lines stand for the cases with and without balloon respectively. For all measurements, adding the balloon in the loop leads to (i) a drop of lost heat power in the upper cold heat exchanger, (ii) a rise of lost heat power in the lower heat exchanger (shown as wide arrow in Figure 4) and (iii) a reduction of total heat lost from the cold heat exchangers. It can be concluded that Gedeon streaming flows in the anticlockwise direction (wide arrows shown in Figure 1) up through the regenerator from hot to cold ends transporting a large amount of heat to the upper cold heat exchanger.

As illustrated in Figure 5, inserting a balloon has no influence on the acoustic pressure amplitudes which could let us suppose that there is no change in the acoustic power at the upper entrance of the regenerator. By use of the first thermodynamic principle over the control volume delimited by he two cold heat exchangers, we calculated an efficiency of the engine (cf. Figure 6 (a)): $\eta=(Q_h-Q_1-Q_2)/Q_h$. Note that heat losses outside the engine (convective and radial), which only depends on temperature levels, can be assumed as identical whenever the balloon is inserted or not (the temperatures levels being not affected by the presence of the balloon – cf. Figure 1 and 2). Thus, we did not take those losses into account in the balance yielding an overestimated

efficiency. It hence can be seen in Figure 6 (b) that the efficiency may be increased by placing the rubber balloon. This let us think that Gedeon streaming indeed exists in our thermoacoustic-Stirling heat engine and that inserting a rubber balloon allows to characterize this phenomenon. Moreover, from the temperatures profiles plotted in Figure 2 and 3 we showed that Gedeon streaming does not affect the temperature levels. Hence, we can imagine that other phenomena are responsible for the profiles curvatures in the regenerator, such as regenerator streaming or acoustic power dissipation in the balloon that could alter the acoustic power at the lower entrance of regenerator.
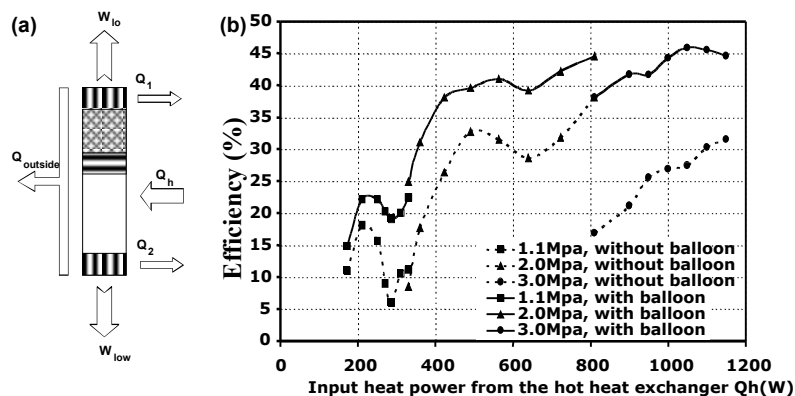

Figure 6. (a) Energy balance for the control volume delimited by the heat exchangers. (b) Efficiency of the thermoacoustic-Stirling heat engine with (solid lines) and without (dashed lines) balloon - radial and convective thermal losses are not taken into account.

CONCLUSION

We have measured temperature profiles in the regenerator and lost heat power carried by water flow in the cold heat exchangers for different working conditions in the presence or not of a rubber balloon inserted in the close-loop resonator. Temperature profiles in the regenerator are not affected by the existence or not of Gedeon streaming leading us to think that another thermal effect predominates in the regenerator. However measurement of heat fluxes through the cold heat exchangers seems to indicate that Gedeon streaming does exist in the engine and that its suppression increases the efficiency. Further quantitative research is required - including radial temperature profile investigation within both the regenerator and the TBT- to place the effect of other streaming losses, e.g., regenerator and Rayleigh streamings.

REFERENCES

1. Gedeon, D.,DC gas flows in Stirling and pulse tube cryocoolers, Cryocoolers (1997) 9 385-390
2. Swift, G.W. , Thermoacoustics: A unifying perspective for some engines and refrigerators, Acoustical Society of America Publications, (2002).
3. Gusev, V., Job, S., Baillet, H., Lotton, P. and Bruneau, M., Acoustic streaming in annular thermoacoustic prime-movers, J. Acoust. Soc. Am (2000) 108(3) 934-945.
4. Hamilton, M.F., Llinskii, Y.A. and Zabolotskaya, E.A., Acoustic streaming generated by standing waves in two-dimensional channels of arbitrary width, JASA (2002) 113(1) 153-160.
5. Swift, G.W., Gardner, D.L. and Backhaus, S., Acoustic recovery of lost power in pulse tube refrigerators, J. Acoust. Soc. Am (1999) 105 711–724.
6. Backhaus, S. and Swift, G.W., A thermoacoustic-Stirling heat engine: Detailed study, J. Acoust. Soc. Am (2000) 107 3148–3166.
7. Backhaus, S. and Swift, G.W., An acoustic streaming instability in thermoacoustic devices utilizing jet pumps, J. Acoust. Soc. Am (2003) 113 1317-1324.
8. Wakeland, R.S. and Keolian, R.M., Influence of velocity profile nonuniformity on minor losses for flow exiting thermoacoustic heat exchangers, J. Acoust. Soc. Am (2002) 1249-1252 .
9. Morris, P. J., Boluriaan, S. and Shieh, C.M., Computational thermoacoustic simulation of minor losses through a sudden contraction and expansion, 7th AIAA/CEAS Aeroacoustics Conference(2001) 2271-2272.
10. Petculescu, A. and Wilen, L., Oscillatory flow in jet pumps: Nonlinear effects and minor losses, J. Acoust. Soc. Am (2003) 113(3) 282-1292
11. Smith, B.L. and Swift, G.W., Power dissipation and time-averaged pressure in oscillating flow through a sudden area change. J. Acoust. Soc. Am (2003) 113 2455-2463.
12. 128 mesh/ (Fr-In) from Gantois.
13. Fabricated by THERMOCOAX
14. Olson, J.R. and Swift, G.W., Acoustic streaming in pulse tube refrigerators: Tapered pulse tube, Cryogenics (1996) 37 769-776.
15. Swift, G.W., Backhaus , S.N., Gardner, D.L., Traveling wave device with mass flux suppression. US Patent (2000) No.6032464.